Available online at www.CivileJournal.org

Civil Engineering Journal

(E-ISSN: 2476-3055; ISSN: 2676-6957)

Vol. 10, No. 03, March, 2024

Influence of Gypsum on the Residual Properties of Fly Ash-Slag-Based Alkali-Activated Concrete

Sandeep G. S. [1], Poornachandra Pandit [1*], Shreelaxmi Prashanth [1*], Jagadisha H. M. [1]

[1] *Department of Civil Engineering, Manipal Institute of Technology, Manipal Academy of Higher Education, Manipal, Karnataka 576104, India.*

Received 14 December 2023; Revised 20 February 2024; Accepted 24 February 2024; Published 01 March 2024

Abstract

High-temperature exposures of concrete lead to serious damage in concrete structures, resulting in the significant decay of mechanical properties and spalling of concrete. Alkali-activated concretes (AAC) of blended aluminosilicate precursors and activators have been proven to have higher thermal endurance than conventional portland cement concrete. Incorporation of gypsum (GY) in alkali-activated systems has proven to positively impact the mechanical properties when adopted in controlled amounts. GY releases SO_4^{2-} to the binder system, which helps in the formation of ettringites, along with Ca^{2+}, which leads to the formation of hydrates. This causes a reduction in porosity and improves strength gain. Incorporation of GY into the fly ash-slag-based alkali-activated system further improves thermal endurance by retaining considerable residual strengths even after 800°C exposure. In the present study, the influence of GY on the residual mechanical properties of fly ash-slag-based AAC is investigated to explore the thermal endurance of the ternary mix at elevated temperatures. The mechanical properties of fly ash (FA), Ground Granulated Blast Furnace Slag (GGBS), and gypsum (GY) ternary blended AAC subjected to elevated temperatures are studied in comparison with conventional portland cement concrete (control mix). AAC design mixes with varying proportions of GY as a replacement to FA-GGBS precursor are tested for mechanical properties to obtain the optimum mix. The residual mechanical properties of the FA-GGBS-GY optimum ternary AAC mix are obtained after exposure to elevated temperatures up to 800°C. The morphology and microstructural characteristics of AAC are studied by Scanning Electron Microscopy (SEM) and Energy-Dispersive X-ray Spectroscopy (EDS) analyses to investigate the influence of gypsum on the thermal endurance of concrete when exposed to elevated temperatures. Improved thermal endurance is observed for AAC when FA-GGBS precursors are replaced with 5% of GY as compared to the thermal endurance of conventional portland cement concrete (PCC) of the same compressive strength.

Keywords: Alkali Activated Concrete (AAC); Fly Ash (FA); Ground Granulated Blast Furnace Slag (GGBS); Gypsum (GY); Elevated Temperature; Microstructure Analysis.

1. Introduction

There is a continuously increasing global demand for cement to meet the necessities and requirements of rapid infrastructure growth. This has necessitated the large-scale usage of cement in recent years. Global production of cement reached 4.1 Gt in 2019 and is expected to grow up to 12–23% by 2050 [1]. It is estimated that approximately 1 ton of CO_2 is released during the production of 1 ton of cement, accounting for about 5% of total global CO_2 emissions [2]. At present, studies are being focused on the 100% replacement of portland cement (PC) with an alternative binder to achieve sustainability in concrete production. Research on the utilization of aluminosilicate-based industrial wastes in concrete production has been trending in recent years. Alkali-activated concrete (AAC) is one of the efficient alternatives that

* Corresponding authors: pc.pandit@manipal.edu; shreelaxmi.p@manipal.edu

http://dx.doi.org/10.28991/CEJ-2024-010-03-017

has the potential to replace conventional portland cement concrete (PCC). In AAC, portland cement is entirely replaced by aluminosilicates or calcium aluminosilicates like coal fly ash, blast furnace slag, metakaolin, silica fume, steel slag, zeolite, etc., and activated using an alkaline activator/s.

Fly ash (FA) is being used as a primary alternative cementitious material all over the world because of its abundance and easy availability [3–6]. More than 196 million tons of FA is being generated in India, which requires considerably large area of land for disposal. Coal-based thermal power plants are the major source of power generation in India to meet the energy demands of the large population. Coal reserves in India are expected to last for more than 100 years [5]. The utilization of FA in sustainable construction is being considered as a primary and effective means of reducing the quantity of FA that is being disposed of on the land as a landfill. AAC with FA as a primary precursor offers similar to superior mechanical and durability characteristics as compared to conventional concrete [7, 8]. The extent of these characteristics largely depends on the source and type of FA as well as the proportions of other blending ingredients used. The usage of FA as a sole precursor in AAC requires heat curing for better and faster polymerization. Also, the mechanical strength attained is moderate. Hence, the addition of calcium aluminosilicates like GGBS to FA in the production of concrete eliminates the demand for heat curing and yields moderately higher strength.

Gypsum (GY) is commonly used in the production of portland cement as a retarding agent. Most of the researchers have studied fly ash, blast furnace slag, steel slag, red mud, metakaolin, and other alumina and/or silica precursor-based binders or mortars to investigate the influence of synthetic gypsums like phosphogypsum (PG) or desulfurized/flue gas desulfurized gypsum (DG). PG is a synthetic gypsum, which is a byproduct of the fertilizer industry produced from phosphate rock, whereas DG is an industrial by-product obtained by desulfurization and purification of flue gas generated after combustion of sulfur-containing fuels (coal, oil, etc.). The phosphorus and fluorine impurities in PG demand careful reuse in concrete production. DG can be used as a substitute for natural gypsum in concrete production. However, there are certain issues and considerations associated with its use in concrete. As DG contains higher levels of sulfates compared to natural gypsum, there is a risk of sulfate attack, compromising its durability and long-term performance. Variations in the chemical composition depending on the source and the specific desulfurization process may cause inconsistencies in the quality of the concrete. Natural gypsum is obtained by mining or quarrying. The total global production of gypsum from mines in 2022 amounted to an estimated 150 million metric tons. The United States is the world's largest producer of crude gypsum and has the world's largest reserves. The abundant gypsum reserves can be utilized in the production of AAC.

In recent years, studies on blended alkali-activated binder systems have gained momentum as they offer improved properties because of the formation of silicate hydrates like calcium aluminosilicate hydrate (C-A-S-H) and sodium aluminosilicate hydrate (N-A-S-H), making the matrix of an alkali-activated system more compact and denser with a refined crack pattern than conventional concrete with a compact pore system [9, 10]. In AAC, hydroxides and silicates of sodium and potassium are commonly used as alkali activators. The gel system formed due to alkali activation in AAC depends on the properties and proportion of precursors along with the activators used. The reaction products from blended systems are complicated and different from those produced when precursors are used in isolation [11, 12]. If the precursor has a low calcium content, like FA (class F), metakaolin, etc., the major chemical reaction products formed are (N-A-S-H). While the high calcium precursors like GGBS, etc. generate (C-A-S-H) as the major reaction product. In the case of blended systems, the predominant chemical reaction products formed are the combination of (C-S-H), (C-A-S-H), and (N-A-S-H) in varying proportions. The proportions of the aforesaid reaction products depend on the proportions of CaO, SiO_2, and Al_2O_3 content in the binders [13–15].

Incorporation of GY into aluminosilicate precursors in alkali-activated materials reduces drying shrinkage and hence enhances dimensional stability [16–18]. The addition of GY has been observed to increase the compressive strength of alkali-activated materials [16, 19, 20]. GY ionizes and releases Ca^{2+} and SO_4^{2-} to a reaction system and is hence expected to improve the performance of the FA-GGBS-based alkali-activated system. However, few studies have shown detrimental effects on compressive strength depending on the proportion of the GY in the binders and the characteristics of the activators used [21–24]. Gypsum has been used as a sulfate activator in FA/slag-based geopolymer pastes, which created favorable conditions for the diffusion and penetration of ions for the activation of FA/slag precursors and led to the formation of ettringite [25]. PG promoted the alkali-activation reaction and reduced setting times when FA/GGBS was partially substituted with phosphogypsum in PG-based alkali-activated binders [26]. A 10% substitution of GGBS with PG in a 50:50 FA/GGBS blend was found to be beneficial. The increased amount of gypsum (up to 15%) in the FA/slag blended pastes was observed to increase pore distribution, which reduced capillary tension and subsequently led to drying shrinkage. Incomplete dissolution of gypsum and a reduction in the formation of ettringites and hydrates were also observed [17]. Optimal strength was obtained with the incorporation of 6% GY of precursor mass content in the FA-slag-based geopolymer cement when a large amount of slag and a small amount of FA were used [27].

The strength properties of FA-GGBS-based alkali-activated materials with DG were optimized by varying curing times and alkali activator modulus. The formation of ettringites due to the incorporation of DG was observed to fill the

tiny micro-cracks, thus forming a denser matrix [28]. DG promoted additional polymerization, ultimately resulting in increased strength in the low-alkaline reaction system. Controlling DG content is recommended to prevent volume filling effect of unreacted DG, which makes the system porous. Modification of the AAC binder matrix for a higher Si/Al ratio offers better residual mechanical strengths after elevated thermal exposures by inhibiting damage due to pore-pressure build-up [29]. When alkali-activated FA and GGBS-based geopolymers are exposed to high temperatures, the sintering reaction heals the micro/meso pores/cracks partially and reduces the adverse impact of re-crystallization on the gel skeleton, leading to the retention of mechanical strength after 600 °C exposure [30]. Higher slag content in the binder induces better mechanical properties to the FA-GGBS-based AAC, but increased brittleness is detrimental to the residual strengths of concrete. FA-based geopolymers offer moderate mechanical properties as compared to FA-GGBS binary systems. Hence, FA and GGBS ratios need to be carefully adopted in the concrete mix to get the advantage of both mechanical properties and better thermal endurance.

Studies on gypsum-based blended concretes are relatively scarce. In general terms, expansion of aggregates and shrinkage of the binder, when the concrete is exposed to elevated temperatures, result in the debonding of aggregates and binder, thus reducing the mechanical and durability properties of concrete. Studies on concrete that mimics real-world applications are needed for societal acceptance.

Concrete is exposed to high temperatures as a building material in various applications like chimneys, metallurgical industries, in case of fire accidents, etc. High-temperature exposures lead to serious damage to concrete structures, resulting in the significant mechanical decay and spalling of concrete. It is essential to adopt high-temperature-resistant concrete for the intended serviceability and to ensure the safety of life. In the present study, FA-GGBS-GY-based ternary blend AAC has been adopted, and residual mechanical properties are investigated at elevated temperatures in comparison with conventional PCC. The study focuses on the use of GY as one of the binders in the FA-GGBS-based ternary system while limiting it to 10% of the total precursor content.

This article presents an investigation on the influence of Gypsum incorporated as a partial substitution for FA-GGBS-based alkali-activated binder systems on the residual properties of FA-GGBS-based AAC. The concrete mix proportions with an alkali-activated FA-GGBS-GY binder system along with the methodology adopted to ascertain the worth of the developed concrete against thermal endurance are presented. The phases developed at each of the elevated temperature levels are presented through micro-analysis. Residual mechanical properties are also tested.

2. Materials

In the present study, FA and GGBS are used as major alkali-activated binder precursors, and the influence of the incorporation of GY as a partial replacement (up to 10%) for FA and GGBS is investigated. The chemical composition of AAC precursors is given in Table 1. SEM images and the elemental composition of AAC precursors and PC are shown in Figure 1. SEM images indicate particles of FA as spherical, GGBS as angular, GY as flaky, and PC as irregularly shaped. A combination of sodium silicate (Na_2SiO_3) and 12M sodium hydroxide (NaOH) alkaline solutions is used as an alkaline activator. M-Sand, used in the present study, conforms to Zone 1 as per IS:383 (1970), with particle sizes ranging between 4.75 mm and 150 µm. The size of coarse aggregates and their proportions in the mix are fixed to match the DIN B grading curve to achieve dense packing [31]. The combined grading of coarse aggregates adopted in the concrete mixes consists of 19% of 20 mm passing, 20% of 12.5 mm passing, 22% of 6.3 mm passing, and 39% of 4.75 mm passing. PC of grade 43 has been used in the control mix. Preliminary tests on PC, precursors, alkaline activator solutions, and aggregates are conducted and reported in Table 2.

Table 1. Chemical composition of AAC precursor materials

Component	FA (%)	GGBS (%)	GY (%)
SiO_2	61.8	40	19.83
Al_2O_3	24.98	4.1	11.63
Fe_2O_3	4.47	2.0	6.20
CaO	3.08	42.0	18.86
MgO	1.77	6.20	5.75
K_2O	0.94	-	1.47
Na_2O	0.28	-	0.05
SO_3	0.31	0.10	43.99
Loss of ignition	1-1.5	0.25	20.36

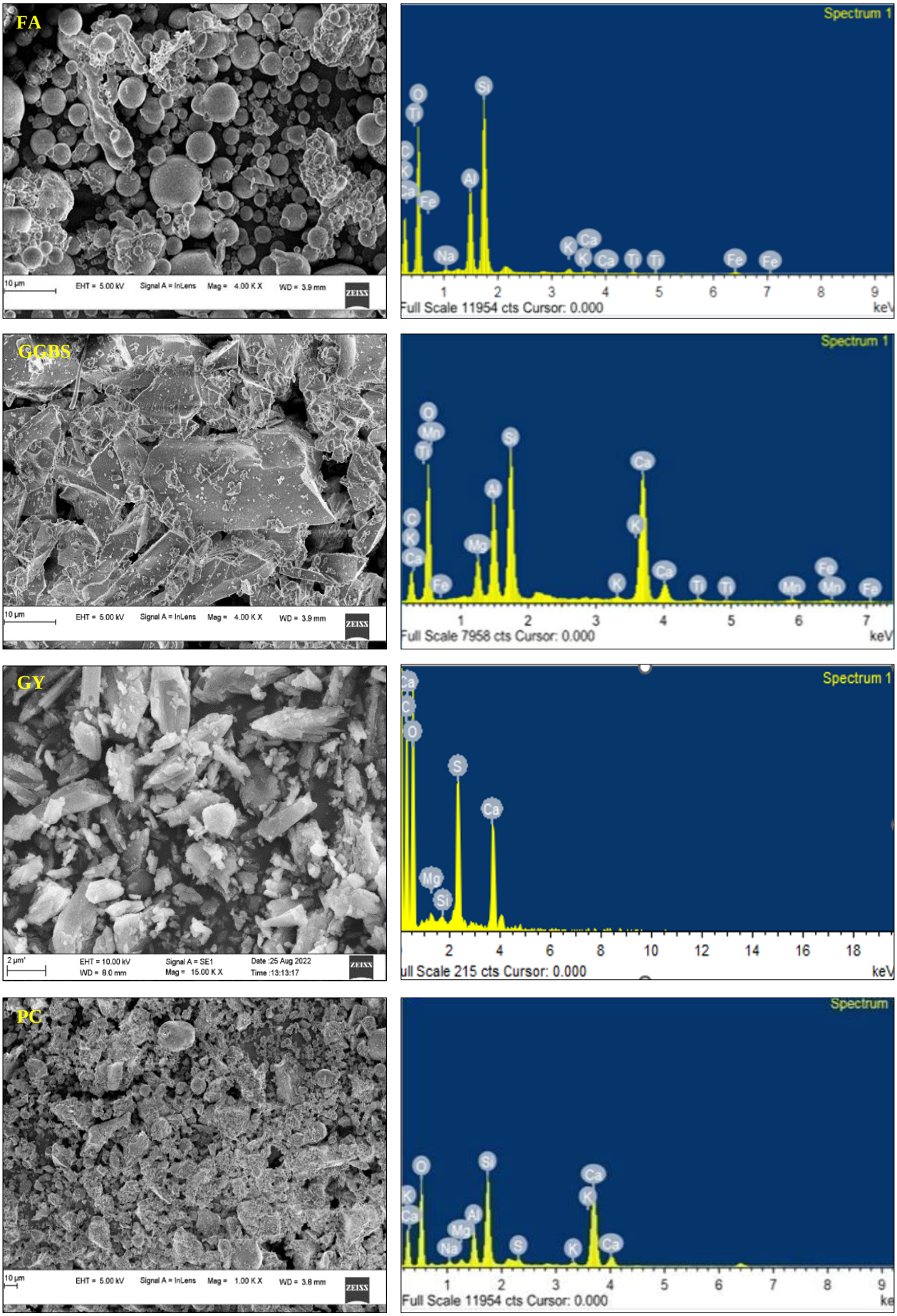

Figure 1. SEM and EDS images of AAC precursors and PC

Table 2. Properties of AAC materials

Physical Property	Raw material	
Specific gravity	FA (Class F)	2.12
	GGBS	2.80
	GY	2.64
	Sodium silicate (Na_2SiO_3) - 46.0% w/w	1.57
	Sodium hydroxide (NaOH) solution – 12M 40.4% w/w	1.46
	Coarse aggregates	2.60
	Fine aggregates	2.60
Fineness modulus	Coarse aggregates	7.76
	Fine aggregates	3.54

3. Research Methodology

The methodology adopted to investigate the influence of GY on the residual properties of FA-GGBS-based AAC in comparison with conventional PCC (control mix) is represented in Figure 2. Alkaline solution content, precursor ratio, activator (Na_2SiO_3 to NaOH) ratio, and NaOH molarity are fixed by conducting trials for designing an AAC mix of required compressive strength and workability [31]. Design mix proportions adopted in casting AAC specimens are given in Table 3. For the preparation of AAC, aggregates and precursors are dry mixed initially in the concrete mixer followed by the addition of activators. Na_2SiO_3 to NaOH activators are prepared at least 24 hours before the mixing time and mixed at least 3 hours before the concrete preparation. Mixing of concrete is continued for 3-5min to get a uniform and workable mix by adding the required amount of water. Alkali-activated ternary mixes are prepared by replacing FA-GGBS precursors with varying percentages of GY in the increments of 2.5% designated as GY0, GY2.5, GY5, GY7.5 and GY10 representing 0%, 2.5%, 5%, 7.5% and 10% replacement respectively. For PCC, 43-grade cement is used, and the concrete mix is designed as per IS:10262 (2019).

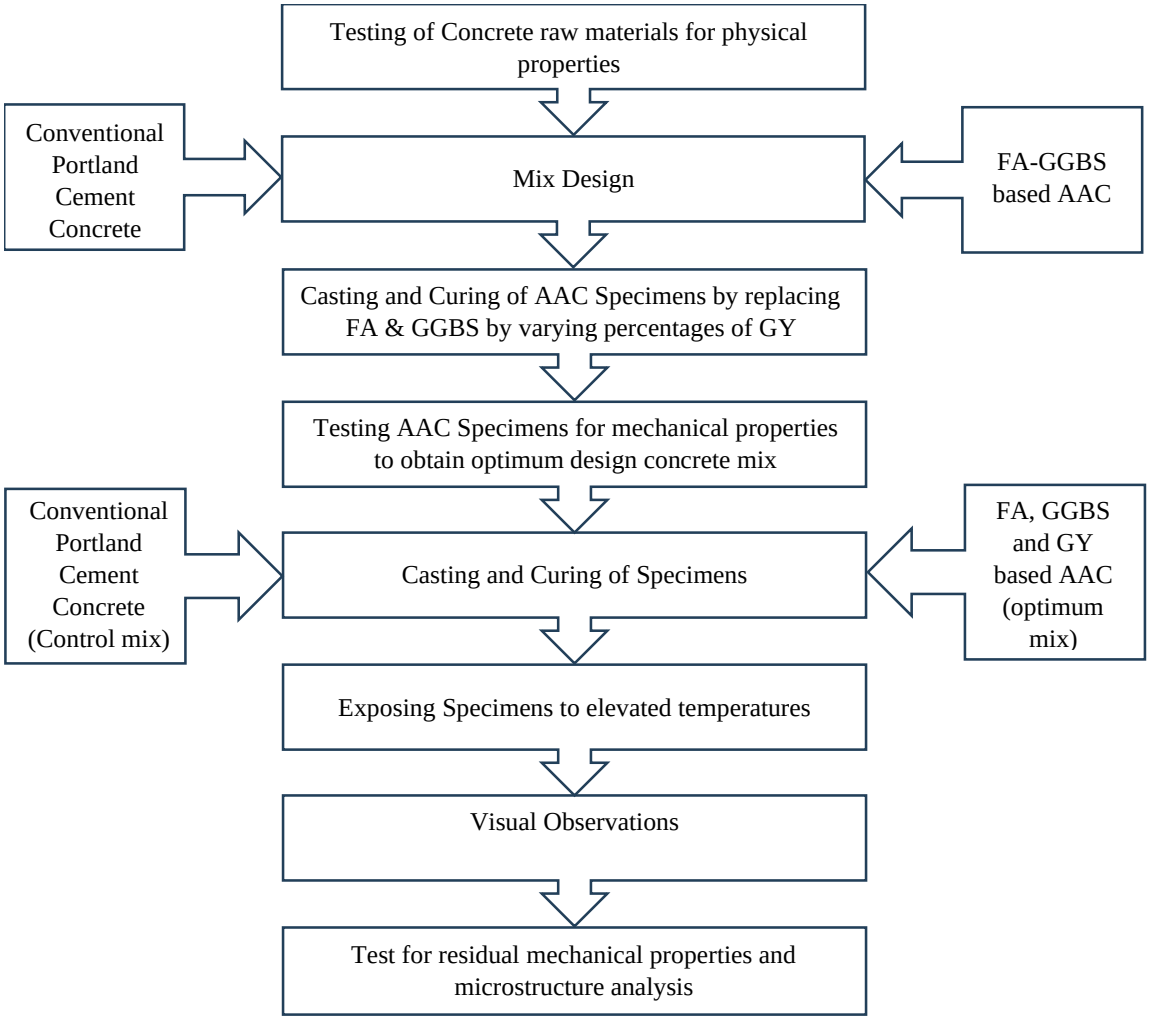

Figure 2. Methodology flow chart of the study

Table 3. Mix Proportions of AAC

Component	GY0	GY2.5	GY5	GY7.5	GY10
FA (class F) in kg/m^3	350	341.25	332.50	323.75	315
GGBS in kg/m^3	150	146.25	142.50	138.75	135
GY in kg/m^3	0	12.50	25	37.50	50
Sodium Hydroxide (NaOH) solution – 12M 40.4% w/w	57 kg/m^3				
Sodium silicate (Na2SiO3) - 46.0% w/w	143 kg/m^3				
Fine aggregates – M sand	667 kg/m^3				
Coarse aggregates	1041 kg/m^3				
(Alkali activator solution / Binder content) ratio	0.4				
Workability	50 mm slump, medium workable concrete				

Cube specimens of size 100 mm, cylinder specimens of 100 mm diameter and 150 mm height, and beam specimens of 150 mm × 100 mm × 100 mm are cast for all AAC mixes and air-cured at room temperature. Specimens are tested for mechanical properties after 7 and 28 days. The optimum AAC mix is obtained by comparing the mechanical strengths of specimens of all AAC mixes. Using optimum AAC mix; cube, beam, and cylinder specimens are cast along with PCC specimens. After 28 days of curing, one set of PCC (water curing) and AAC (air curing) specimens are tested for mechanical strengths. Another set of specimens is exposed to elevated temperatures of up to 800°C in an electric furnace. The temperature in the furnace is raised at a constant rate of 5.5°C/min. After reaching the designated temperature (200°C, 400°C, 600°C and 800°C), specimens are retained for 2 hours in the furnace [29]. After 2 hours of retention time, the furnace is switched off and allowed to cool down until room temperature is reached. The Specimens are taken out of the furnace and tested for residual strengths. Binder samples extracted from the AAC and PCC specimens after elevated temperature exposures are subjected to Scanning Electron Microscopy (SEM) and Energy-Dispersive X-ray Spectroscopy (EDS) analyses.

4. Results and Discussions

AAC specimens with varying percentages of GY are tested for compressive, tensile, and flexure strengths to obtain an AAC mix with the optimum percentage of GY. Concrete specimens with the optimum percentage of GY are then exposed to elevated temperatures to obtain the residual strengths to investigate the influence of GY on AAC. Chemical reactions between FA, GGBS, and GY led to the formation of new complex crystalline products. A few unreacted compounds of precursors are also found throughout the process of alkali activation.

4.1. The Optimum Percentage of GY as a Replacement for FA-GGBS in AAC

AAC mixes are prepared by replacing FA and GGBS with GY at varying percentages (0%, 2.5%, 5%, 7.5%, and 10%). Figure 3 shows the influence of GY on the compressive, split tensile, and flexure strengths of AAC at 7 and 28 days. Positive impact up to 5% replacement and negative impact with the increase in the percentage of replacement from 5% to 10% is observed.

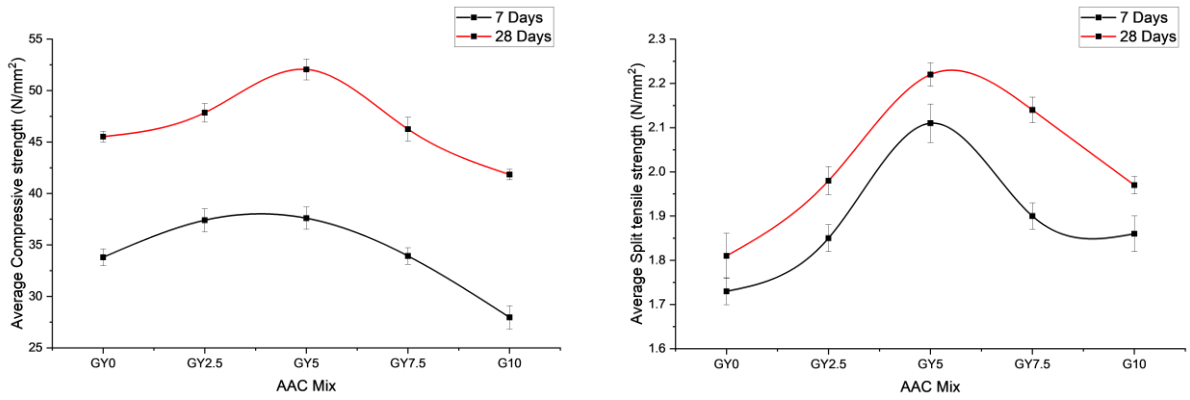

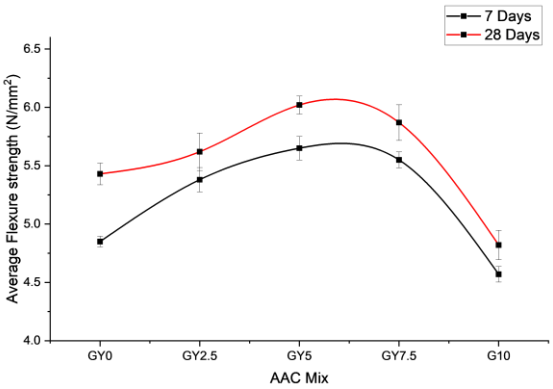

Figure 3. Variation in mechanical strengths of AAC with varying GY content at 7 and 28 days

The mechanical strengths of all AAC mixes considered for the study are tabulated in Table 4. GY5 attained 14.34%, 12.27%, and 11.07% higher compressive, split tensile, and flexure strengths respectively at 28 days than GY0. As compared to GY5, compressive, split tensile, and flexure strengths of GY7.5 are reduced by 11.14%, 3.6%, and 2.49% respectively, and 19.62%, 11.26%, and 19.93% respectively for GY10 AAC mix. According to strength tests, the AAC mix with 5% GY possessed higher mechanical strengths than the control AAC mix, GY0. However, the addition of GY beyond 5% decreased the strength of AAC. Similar results were reported in earlier studies with FA and PG [32]. Based on this observation, GY5 is considered as the optimum mix for elevated temperature exposures.

Table 4. Mechanical strengths of AAC with varying GY content at 7 and 28 days

AAC Mix	Average Compressive strength in N/mm²		Average Split tensile strength in N/mm²		Average flexure strength in N/mm²	
	7 days	28 days	7 days	28 days	7 days	28 days
GY0	33.8	45.52	1.73	1.81	4.85	5.43
GY2.5	37.4	47.85	1.85	1.98	5.38	5.62
GY5	37.6	52.05	2.11	2.22	5.65	6.02
GY7.5	33.93	46.25	1.90	2.14	5.55	5.87
GY10	27.96	41.84	1.86	1.97	4.57	4.82

Binders extracted from GY0, GY2.5, GY5, GY7.5, and GY10 AAC specimens are subjected to microstructure analysis and surface morphology is observed. SEM images of all samples considered for the study are shown in Figure 4. The chemical reactions of the ternary blend alkali activation process are complex. They involve dissolution, polymerization, and subsequent reformation of various silicate, aluminate, and calcium-based compounds. These reactions resulted in new phases, which helped to develop the strength, durability, and overall performance of AAC. The alkalis in the activator solution (NaOH and Na_2SiO_3) led to the dissolution and release of (Si^{2+}) and (Al^{3+}) from the FA. Similarly, under the action of alkalis, (Ca^{2+}) and (SiO_4^{4-}) ions were released from GGBS. Released ions combined with alkali metal ions and generated gel-like crystalline structures, primarily composed of calcium silicate hydrate (C-S-H), calcium aluminosilicate hydrate (C-A-S-H), Sodium aluminosilicate hydrate (N-A-S-H) and other compounds by polymerization in FA-GGBS-based AAC which contributed to the binding properties and strength gain in AAC [33]. GY, predominantly composed of calcium sulfate dihydrate, contributes calcium (Ca^{2+}) ions to the system in the presence of alkalis.

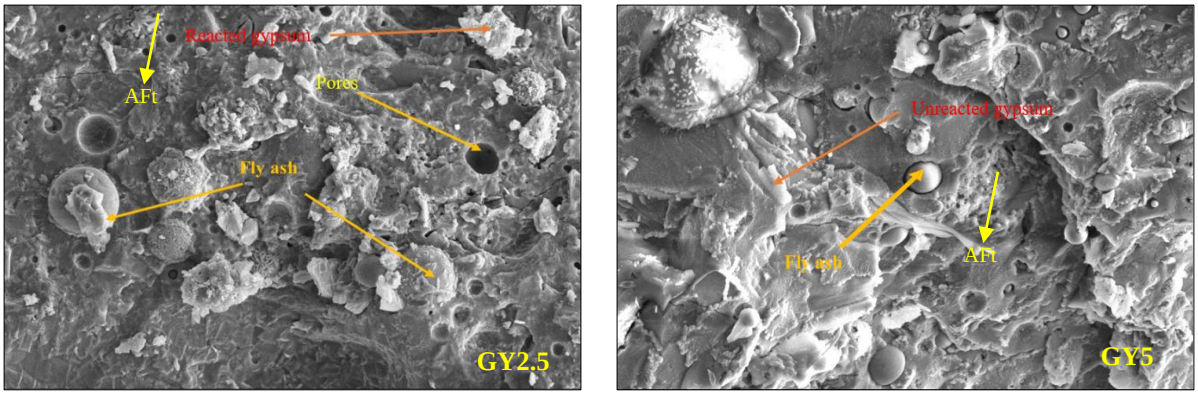

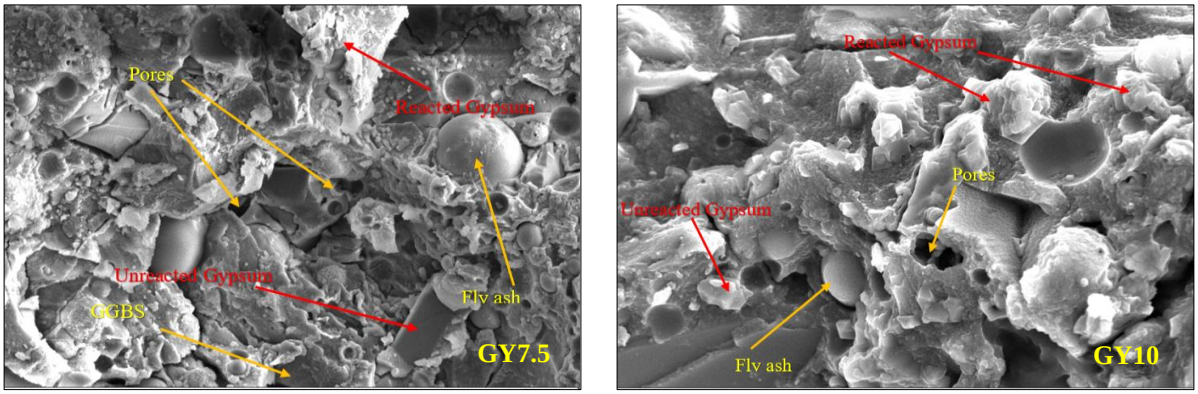

Figure 4. SEM images of AAC with varying GY content

GY in AAC ternary binder released (SO_4^{2-}) ions into the binder paste. Dissolved (Ca^{2+}) and (SO_4^{2-}) ions in the FA-GGBS-GY blend, combined with transformed aluminium hydroxide $[Al(OH)_6]^{3-}$ to form ettringite (AFt). These needle-shaped AFt crystals reduced the porosity by filling the pores, thus improving the strength [34]. Thus (C-S-H), (C-A-S-H), (N-A-S-H), and AFt are responsible for dense microstructure leading to the strength gain when GY content was ≤5%. With the increase in GY content to 7.5% and 10%, the formation of excessive AFt led to the destruction of the gel structure of AAC binders due to the volume expansion leading to increased porosity. This increased porosity subsequently led to the deterioration of the strength. Similar results were obtained in an earlier study with Desulfurization gypsum [33]. Additionally, since a certain percentage of FA-GGBS is replaced with GY, the formation of reaction products is reduced due to the lower dissolution rate of (Ca^{2+}), (Si^{2+}), and (Al^{3+}) ions. Higher $CaSO_4$ content has been proven to cause adverse effects on the formation of the (C-S-H), (C-A-S-H), and (N-A-S-H) gel [17]. SEM images of GY7.5 and GY10 AAC shown in Figure 4 indicate the existence of a considerable number of pores and unreacted precursors than GY5 AAC indicating the adverse effect of AFt and incomplete dissolution of precursors in the activator solution respectively. These are responsible for the reduction in strengths because of an increase in porosity and lesser gel formation. A larger amount of GY acts as a barrier for the formation of reaction products which reduces the cohesion in the microstructure resulting in the reduction of mechanical strengths.

Elements and elemental ratios of different AAC mixes considered for the study are listed in Table 5. An increase in the ratios of (Ca/Si), (Si/Al), (Na/Al), (Ca/(Si+Al)), and (Na/(Si+Al)) is observed with the increase in the replacement of GY with FA-GGBS up to 5% and decrease is observed with further increase in the GY replacement. Increase in the ratios of (Ca/Si), (Si/Al), (Na/Al), (Ca/(Si+Al)), and (Na/(Si+Al)) is observed from 0.769, 2.252, 0.83, 0.533, and 0.255 to 1.204, 2.990, 0.908, 0.902, and 0.228 respectively for G5 AAC mix w.r.t GY0. Higher (Ca/Si), Ca/(Si+Al), and (Na/(Si+Al)) ratios of a mix indicate a higher rate of polymerization due to enhanced dissolution of precursors leading to the formation of denser reaction products. (Ca/Si) and (Ca/(Si+Al)) ratios dominate over (Na/(Si+Al)) ratio for G5 AAC which indicate (C-S-H) and (C-A-S-H) as major crystalline reaction products formed. (Si/Al) ratio is the most critical factor for residual properties in the AAC system at elevated temperatures and the mix with a higher (Si/Al) ratio offers better resistance to elevated temperature exposures [35–37]. G5 AAC with high elemental ratios, high (Si/Al) ratio, and relatively better mechanical properties as compared to other mixes considered for the study is adopted as the optimum mix for elevated temperature exposures.

Table 5. EDS analysis of AAC samples at ambient temperature

AAC Mix	Elements (% by wt.) and their ratio								
	Na	Ca	Si	Al	Ca/Si	Si/Al	Na/Al	Ca/(Si+Al)	Na/(Si+Al)
GY0	5.33	11.13	14.46	6.42	0.769	2.252	0.830	0.533	0.255
GY2.5	2.01	8.93	10.50	3.83	0.850	2.741	0.525	0.624	0.140
GY5	3.65	14.48	12.02	4.02	1.204	2.990	0.908	0.902	0.288
GY7.5	2.72	10.50	12.96	4.90	0.810	2.644	0.555	0.587	0.152

4.2. Residual Mechanical Strengths of PCC and G5 AAC

Specimens are exposed to elevated temperatures after 28 days of ambient temperature curing for G5 AAC and water curing for PCC specimens. Electric furnace temperature is gradually increased at a constant rate of 5.5°C/min till the designated temperature i.e., 200°C, 400°C, 600°C, and 800°C is reached. Specimens are retained for 2 hours at the

designated temperature. After retention time, the furnace is switched off and allowed to cool until room temperature is reached. The specimens are taken out of the furnace and tested for mechanical strengths to investigate the influence of GY on the residual properties of FA-GGBS-GY-based AAC as compared to PCC.

The visual appearances of G5 AAC and PCC specimens after exposure to elevated temperatures are shown in Figures 5 and 6. Surface layers of PCC specimens are seen to be disintegrated and spalled off on 800^0C exposures. PCC specimens suffered a higher level of disintegration at elevated temperatures as compared to AAC specimens due to the early loss of bond between binder and aggregates because of considerable dehydration; and because of early gel structure disintegration. The binder matrix in AAC appeared to be more stable and denser than PCC binder offering better resistance to exposed elevated temperatures.

Figure 5. Concrete specimens after exposure to 800℃

Figure 6. The visual appearance of G5 AAC and PCC beam specimens after exposure to 400℃

Variations in the mechanical strengths of PCC and G5 AAC specimens at elevated temperature exposures from 200℃ to 800℃ are shown in Figure 7. Residual mechanical strengths of PCC and G5 AAC specimens after exposure to elevated temperatures relative to their mechanical strengths at ambient temperature are tabulated in Table 6. AAC specimens showed higher residual mechanical properties than PCC specimens at every exposure temperature considered. Maximum reduction in compressive strength is observed between 600℃-800℃ for PCC specimens and between 400℃-600℃ for G5 AAC specimens. Similarly, PCC and G5 AAC specimens lost maximum split tensile and flexure strengths between 200℃-400℃. After exposure to 800℃ exposure, G5 AAC specimens retained considerable mechanical properties to an extent of 25% to 47%, whereas PCC specimens lost almost 85% to 100% w.r.t ambient strengths. At 800℃, the relative residual compressive, split tensile, and flexure strengths of PCC specimens w.r.t mechanical strengths at ambient temperature are observed to be 0.15, 0.01, and 0 as compared to 0.53, 0.2, and 0.25 respectively for G5 AAC specimens. Lower cracking and spalling, and higher residual mechanical strengths of G5 AAC at higher temperature exposures indicate their better performance and hence are considered to offer excellent endurance at elevated temperature exposures as compared to PCC.

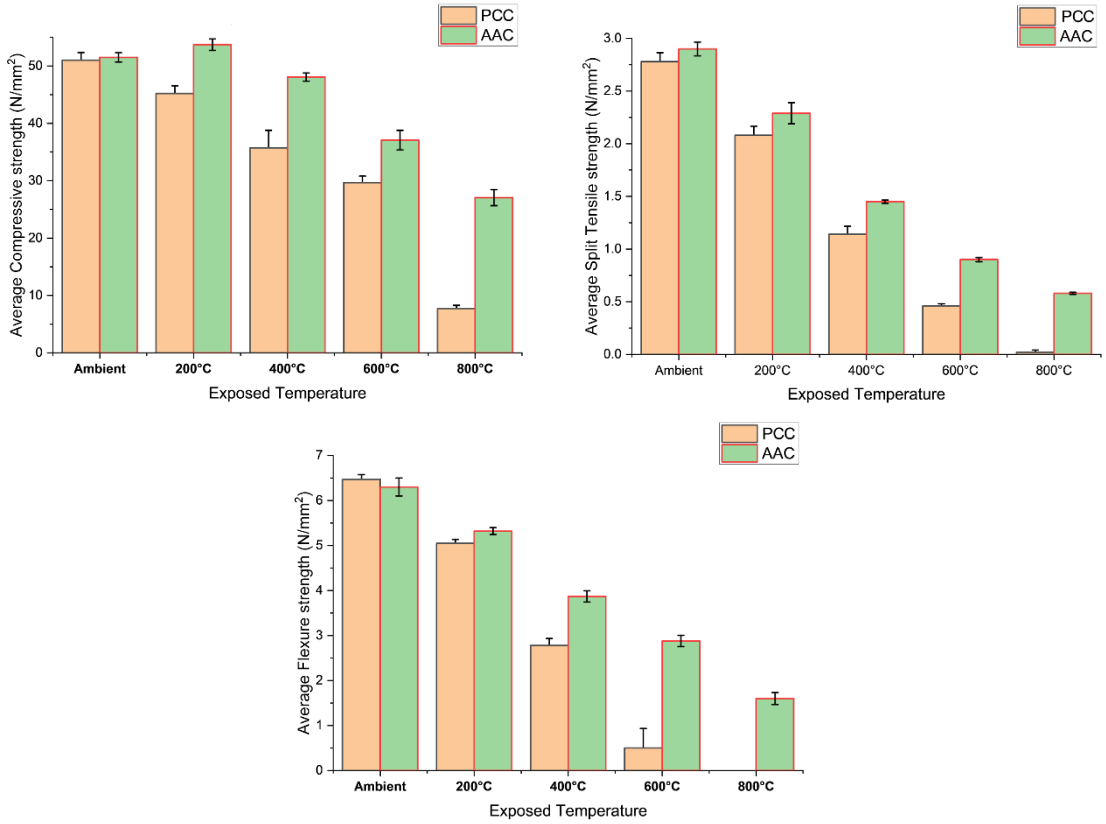

Figure 7. Residual mechanical strengths of PCC and G5 AAC specimens at different elevated temperature exposures

Table 6. Residual mechanical strengths of specimens after exposure to elevated temperatures relative to mechanical strengths at ambient temperature

	Specimens	Exposure temperature			
	Al	200 ºC	400 ºC	600 ºC	800 ºC
Relative residual compressive strengths	PCC	0.89	0.70	0.58	0.15
	G5 AAC	1.04	0.94	0.72	0.53
Relative residual split tensile strengths	PCC	0.75	0.41	0.17	0.01
	G5 AAC	0.79	0.50	0.31	0.20
Relative residual flexure strengths	PCC	0.78	0.43	0.08	0
	G5 AAC	0.85	0.61	0.46	0.25

From the SEM images of G5 AAC in Figure 8, no cracks are visible at 800°C, and minor cracks are visible at 600°C exposure. This is due to the sintering of hydrates and unreacted precursor particles which resulted in the greater inter-particle connectivity between 600°C-800°C [29]. Sintering of hydrates in G5 AAC filled up micro to macro cracks formed on exposure to elevated temperatures up to around 800°C. This in turn helped in the retention of residual mechanical strengths at elevated temperature exposures.

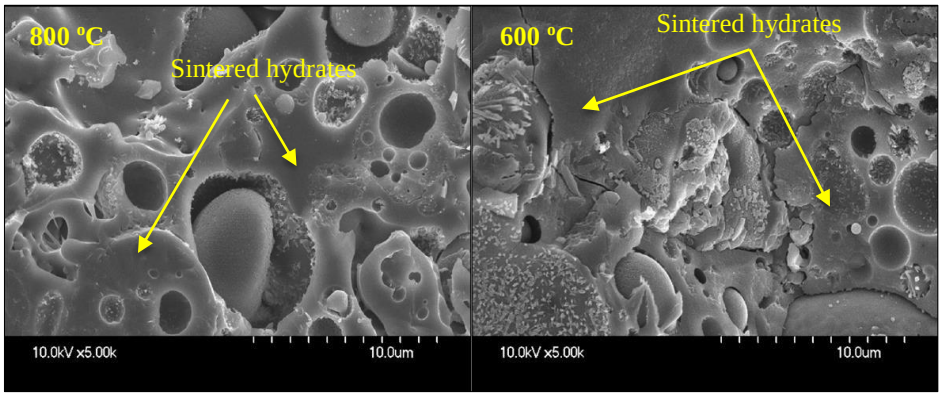

Figure 8. SEM images of G5 AAC specimens after exposure to 600°C and 800°C

EDS analysis results of PCC and G5 AAC samples are shown in Tables 7 and 8 respectively. Reduction in (Ca/Si) and (Si/Al) ratios of PCC with the increase in exposure temperature from 200°C to 800°C is observed due to the decomposition and disintegration of (C-S-H) gel which resulted in the loss of mechanical strengths. An increase in the elemental ratios of G5 AAC with the increase in exposure temperature up to 200°C is observed due to the enhanced polymerization which resulted in the increased mechanical strengths as per Table 6. At different elevated temperatures the specimens are exposed to, in the present study, the elemental ratios of G5 AAC are higher than those of PCC. This indicates a higher amount of thermal degradation of PCC gel structure than G5 AAC and thus justifies higher thermal endurance of G5 AAC than PCC with considerable residual strengths at elevated temperatures. This behavior proves G5 AAC mix is a better alternative to PCC for elevated temperature exposure applications up to 800°C.

Table 7. EDS analysis of PCC samples after exposure to elevated temperatures

Exposure Temperature	Elements (% by wt.) and their ratio				
	Ca	Si	Al	Ca/Si	Ca/(Si+Al)
Ambient	12.57	9.67	12.08	1.30	0.80
200ºC	6.15	7.88	11.76	0.78	0.67
400ºC	2.99	5.45	9.40	0.55	0.58
800ºC	2.46	5.12	11.63	0.48	0.44

Table 8. EDS analysis of G5 AAC samples after exposure to elevated temperatures

Exposure Temperature	Elements (% by wt.) and their ratio								
	Na	Ca	Si	Al	Ca/Si	Si/Al	Na/Al	Ca/(Si+Al)	Na/(Si+Al)
Ambient	13.41	17.55	9.00	9.38	1.95	0.96	1.43	0.96	0.73
200ºC	16.74	25.97	12.92	11.24	2.01	1.15	1.49	1.08	0.69
400ºC	9.34	11.29	6.45	7.59	1.75	0.85	1.23	0.80	0.67
800ºC	5.82	5.34	3.40	6.54	1.57	0.52	0.89	0.54	0.59

5. Conclusions

- Partial replacement of FA-GGBS precursors with 5% GY in an alkali activation system is found to be beneficial in improving the mechanical properties of AAC. The microstructures of the FA-GGBS-GY ternary blended concrete showed better thermal endurance as compared to PCC and hence is a potential alternative for elevated temperature applications.
- The optimum mix design of FA-GGBS-GY-based AAC is obtained by replacing FA-GGBS (70:30) with 5% GY. The formation of ettringite (AFt) crystals filled up the initial pores and improved mechanical strength. With the increase in GY content to 7.5% and 10%, excessive ettringite (AFt) formed led to the destruction of the gel structure due to the volume expansion. This increased the porosity and deteriorated the strength.
- GY5 AAC specimens showed higher residual mechanical properties than PCC specimens at every elevated exposure temperature considered. GY5 AAC specimens offered higher resistance to spalling and cracking than PCC specimens and retained better residual mechanical properties on elevated temperature exposures up to 800℃.
- At every elevated temperature exposure considered in the present study, between 200℃ to 800℃, the elemental ratios of GY5 AAC are higher than those of PCC. This indicates a higher amount of thermal degradation of PCC gel structure than GY5 AAC. Strong gel structure, sintering of unreacted precursor particles and binder matrix at higher temperatures in AAC helped in retaining considerable residual mechanical strengths than PCC even after exposure to elevated temperatures up to 800℃. This justifies better-elevated temperature endurance of Fly ash-slag-gypsum-based AAC than PCC.

6. Declarations

6.1. Author Contributions

Conceptualization, S.G., P.P., and S.P.; methodology, S.G. and J.H.; formal analysis, S.G. and J.H.; investigation, S.G.; resources, S.G.; data curation, S.G.; writing—original draft preparation, S.G.; writing—review and editing, S.G., S.P., P.P., and J.H.; visualization, S.G. and J.H.; supervision, S.G. and J.H.; project administration, S.G.; funding acquisition, S.G. All authors have read and agreed to the published version of the manuscript.

6.2. Data Availability Statement

The data presented in the study are available in the article.

6.3. Funding

The article publishing charges was provided by Manipal Academy of Higher Education, Manipal, Karnataka, India.

6.4. Conflicts of Interest

The authors declare no conflict of interest.

7. References

[1] Guo, Y., Luo, L., Liu, T., Hao, L., Li, Y., Liu, P., & Zhu, T. (2024). A review of low-carbon technologies and projects for the global cement industry. Journal of Environmental Sciences (China), 136, 682–697. doi:10.1016/j.jes.2023.01.021.

[2] Plaza, M. G., Martínez, S., & Rubiera, F. (2020). Co2 capture, use, and storage in the cement industry: State of the art and expectations. Energies, 13(21). doi:10.3390/en13215692.

[3] Farooq, F., Jin, X., Faisal Javed, M., Akbar, A., Izhar Shah, M., Aslam, F., & Alyousef, R. (2021). Geopolymer concrete as sustainable material: A state of the art review. Construction and Building Materials, 306. doi:10.1016/j.conbuildmat.2021.124762.

[4] Provis, J. L., Palomo, A., & Shi, C. (2015). Advances in understanding alkali-activated materials. Cement and Concrete Research, 78, 110–125. doi:10.1016/j.cemconres.2015.04.013.

[5] Rastogi, A., & Paul, V. K. (2020). A critical review of the potential for fly ash utilisation in construction-specific applications in India. Environmental Research, Engineering and Management, 76(2), 65–75. doi:10.5755/J01.EREM.76.2.25166.

[6] Zhuang, X. Y., Chen, L., Komarneni, S., Zhou, C. H., Tong, D. S., Yang, H. M., Yu, W. H., & Wang, H. (2016). Fly ash-based geopolymer: Clean production, properties and applications. Journal of Cleaner Production, 125, 253–267. doi:10.1016/j.jclepro.2016.03.019.

[7] Pradhan, P., Dwibedy, S., Pradhan, M., Panda, S., & Panigrahi, S. K. (2022). Durability characteristics of geopolymer concrete - Progress and perspectives. Journal of Building Engineering, 59. doi:10.1016/j.jobe.2022.105100.

[8] Singh, B., Ishwarya, G., Gupta, M., & Bhattacharyya, S. K. (2015). Geopolymer concrete: A review of some recent developments. Construction and Building Materials, 85, 78–90. doi:10.1016/j.conbuildmat.2015.03.036.

[9] Mehta, A., Siddique, R., Ozbakkaloglu, T., Uddin Ahmed Shaikh, F., & Belarbi, R. (2020). Fly ash and ground granulated blast furnace slag-based alkali-activated concrete: Mechanical, transport and microstructural properties. Construction and Building Materials, 257. doi:10.1016/j.conbuildmat.2020.119548.

[10] Kamath, M., Prashant, S., & Kumar, M. (2021). Micro-characterisation of alkali activated paste with fly ash-GGBS-metakaolin binder system with ambient setting characteristics. Construction and Building Materials, 277. doi:10.1016/j.conbuildmat.2021.122323.

[11] Lecomte, I., Henrist, C., Liégeois, M., Maseri, F., Rulmont, A., & Cloots, R. (2006). (Micro)-structural comparison between geopolymers, alkali-activated slag cement and Portland cement. Journal of the European Ceramic Society, 26(16), 3789–3797. doi:10.1016/j.jeurceramsoc.2005.12.021.

[12] Wang, X. Y., & Lee, H. S. (2010). Modeling the hydration of concrete incorporating fly ash or slag. Cement and Concrete Research, 40(7), 984–996. doi:10.1016/j.cemconres.2010.03.001.

[13] Castellote, M., Alonso, C., Andrade, C., Castro, P., & Echeverría, M. (2001). Calorimetric study of alkaline activation of calcium hydroxide-metakaolin solid mixtures. Cement and Concrete Research, 31(2), 25–30. doi:10.1016/S0008-8846(00)00435-X.

[14] Ruiz-Santaquiteria, C., Fernández-Jiménez, A., & Palomo, A. (2016). Alternative prime materials for developing new cements: Alkaline activation of alkali aluminosilicate glasses. Ceramics International, 42(8), 9333–9340. doi:10.1016/j.ceramint.2016.03.111.

[15] Garcia-Lodeiro, I., Palomo, A., Fernández-Jiménez, A., & MacPhee, D. E. (2011). Compatibility studies between N-A-S-H and C-A-S-H gels. Study in the ternary diagram Na2O-CaO-Al2O3-SiO 2-H2O. Cement and Concrete Research, 41(9), 923–931. doi:10.1016/j.cemconres.2011.05.006.

[16] Chang, J. J., Yeih, W., & Hung, C. C. (2005). Effects of gypsum and phosphoric acid on the properties of sodium silicate-based alkali-activated slag pastes. Cement and Concrete Composites, 27(1), 85–91. doi:10.1016/j.cemconcomp.2003.12.001.

[17] Son, H., Park, S. M., Seo, J. H., & Lee, H. K. (2019). Effect of CaSO4 incorporation on pore structure and drying shrinkage of alkali-activated binders. Materials, 12(10). doi:10.3390/MA12101673.

[18] Hanjitsuwan, S., Injorhor, B., Phoo-ngernkham, T., Damrongwiriyanupap, N., Li, L. Y., Sukontasukkul, P., & Chindaprasirt, P. (2020). Drying shrinkage, strength and microstructure of alkali-activated high-calcium fly ash using FGD-gypsum and dolomite as expansive additive. Cement and Concrete Composites, 114. doi:10.1016/j.cemconcomp.2020.103760.

[19] Ghosh, A., & Subbarao, C. (2001). Microstructural Development in Fly Ash Modified with Lime and Gypsum. Journal of Materials in Civil Engineering, 13(1), 65–70. doi:10.1061/(asce)0899-1561(2001)13:1(65).

[20] Jeong, Y., Park, H., Jun, Y., Jeong, J. H., & Oh, J. E. (2016). Influence of slag characteristics on strength development and reaction products in a CaO-activated slag system. Cement and Concrete Composites, 72, 155–167. doi:10.1016/j.cemconcomp.2016.06.005.

[21] Yoon, S., Park, H., Yum, W. S., Suh, J. Il, & Oh, J. E. (2018). Influence of calcium sulfate type on evolution of reaction products and strength in NaOH- and CaO-activated ground granulated blast-furnace slag. Applied Sciences, 8(12), 2500. doi:10.3390/app8122500.

[22] Wang, D., Wang, Q., & Huang, Z. (2020). New insights into the early reaction of NaOH-activated slag in the presence of CaSO4. Composites Part B: Engineering, 198. doi:10.1016/j.compositesb.2020.108207.

[23] An, Q., Pan, H., Zhao, Q., Du, S., & Wang, D. (2022). Strength development and microstructure of recycled gypsum-soda residue-GGBS based geopolymer. Construction and Building Materials, 331. doi:10.1016/j.conbuildmat.2022.127312.

[24] Hamdan, A., Song, H., Yao, Z., Alnahhal, M. F., Kim, T., & Hajimohammadi, A. (2023). Modifications to reaction mechanisms, phase assemblages and mechanical properties of alkali-activated slags induced by gypsum addition. Cement and Concrete Research, 174. doi:10.1016/j.cemconres.2023.107311.

[25] Cong, P., & Mei, L. (2021). Using silica fume for improvement of fly ash/slag based geopolymer activated with calcium carbide residue and gypsum. Construction and Building Materials, 275. doi:10.1016/j.conbuildmat.2020.122171.

[26] Feng, Y., Xue, Z., Zhang, B., Xie, J., Chen, C., Tan, J., & Zhao, C. (2023). Effects of phosphogypsum substitution on the performance of ground granulated blast furnace slag/fly ash-based alkali-activated binders. Journal of Building Engineering, 70. doi:10.1016/j.jobe.2023.106387.

[27] Wang, Y., Huo, H., Chen, B., & Cui, Q. (2023). Development and optimization of phosphogypsum-based geopolymer cement. Construction and Building Materials, 369. doi:10.1016/j.conbuildmat.2023.130577.

[28] Luan, Y., Wang, J., Ma, T., Wang, S., & Li, C. (2023). Modification mechanism of flue gas desulfurization gypsum on fly ash and ground granulated blast-furnace slag alkali-activated materials: Promoting green cementitious material. Construction and Building Materials, 396. doi:10.1016/j.conbuildmat.2023.132400.

[29] Tu, W., & Zhang, M. (2023). Behaviour of alkali-activated concrete at elevated temperatures: A critical review. Cement and Concrete Composites, 138. doi:10.1016/j.cemconcomp.2023.104961.

[30] Luo, Y., Li, S. H., Klima, K. M., Brouwers, H. J. H., & Yu, Q. (2022). Degradation mechanism of hybrid fly ash/slag based geopolymers exposed to elevated temperatures. Cement and Concrete Research, 151. doi:10.1016/j.cemconres.2021.106649.

[31] Reddy, M. S., Dinakar, P., & Rao, B. H. (2018). Mix design development of fly ash and ground granulated blast furnace slag based geopolymer concrete. Journal of Building Engineering, 20, 712–722. doi:10.1016/j.jobe.2018.09.010.

[32] Rashad, A. M. (2015). Potential use of phosphogypsum in alkali-activated fly ash under the effects of elevated temperatures and thermal shock cycles. Journal of Cleaner Production, 87(1), 717–725. doi:10.1016/j.jclepro.2014.09.080.

[33] Wang, J., Ma, T., Luan, Y., Wang, S., & Zhang, Y. (2023). Investigation on the effects of desulfurization gypsum on the engineering properties of ternary geopolymers: Improving the utilization of industrial wastes. Journal of Cleaner Production, 414. doi:10.1016/j.jclepro.2023.137638.

[34] Li, Y., Liu, X., Li, Z., Ren, Y., Wang, Y., & Zhang, W. (2021). Preparation, characterization and application of red mud, fly ash and desulfurized gypsum based eco-friendly road base materials. Journal of Cleaner Production, 284. doi:10.1016/j.jclepro.2020.124777.

[35] Thokchom, S., Mandal, K. K., & Ghosh, S. (2012). Effect of Si/Al Ratio on Performance of Fly Ash Geopolymers at Elevated Temperature. Arabian Journal for Science and Engineering, 37(4), 977–989. doi:10.1007/s13369-012-0230-5.

[36] Lahoti, M., Wong, K. K., Yang, E. H., & Tan, K. H. (2018). Effects of Si/Al molar ratio on strength endurance and volume stability of metakaolin geopolymers subject to elevated temperature. Ceramics International, 44(5), 5726–5734. doi:10.1016/j.ceramint.2017.12.226.

[37] He, R., Dai, N., & Wang, Z. (2020). Thermal and Mechanical Properties of Geopolymers Exposed to High Temperature: A Literature Review. Advances in Civil Engineering, 2020. doi:10.1155/2020/7532703.